







Spatial variability of soil hydraulic conductivity and runoff generation types in a small mountainous catchment


YANG Yong¹  <https://orcid.org/0000-0002-6124-6165>; e-mail: yy177@lzb.ac.cn

CHEN Ren-sheng^{1,2*}  <https://orcid.org/0000-0002-2073-3098>;  e-mail: crs2008@lzb.ac.cn

SONG Yao-xuan¹  <https://orcid.org/0000-0002-8913-9580>; e-mail: yxsdesert@163.com

HAN Chun-tan¹  <https://orcid.org/0000-0002-8412-6692>; e-mail: hancht@lzb.ac.cn

LIU Zhang-wen¹  <https://orcid.org/0000-0002-2791-9653>; e-mail: zwliu@lzb.ac.cn

LIU Jun-feng¹  <https://orcid.org/0000-0002-4773-0786>; e-mail: liujfzyou@lzb.ac.cn

*Corresponding author

¹ Qilian Alpine Ecology and Hydrology Research Station, Key Laboratory of Ecohydrology Inland River Basin, Northwest Institute of Eco-Environment and Resources, Chinese Academy of Sciences, Lanzhou 730000, China

² College of Urban and Environmental Sciences, Northwest University, Xi'an 710127, China

Citation: Yang Y, Chen RS, Song YX, et al. (2020) Spatial variability of soil hydraulic conductivity and runoff generation types in a small mountainous catchment. *Journal of Mountain Science* 17(11). <https://doi.org/10.1007/s11629-020-6258-1>

© Science Press, Institute of Mountain Hazards and Environment, CAS and Springer-Verlag GmbH Germany, part of Springer Nature 2020

Abstract: As an important soil property, saturated hydraulic conductivity (K_s) controls many hydrological processes, such as runoff generation types, soil moisture storage and water movement. Because of the extremely harsh natural environmental conditions and soil containing a significant fraction of gravel fragments in high-elevation mountainous catchments, the measurement data of K_s and other soil properties are seriously lacking, which leads to poor understanding on its hydrological processes and water cycle. In this study, the vertical variation (0–150 cm) of K_s and other soil properties from 38 soil profiles were measured under five different land cover types (alpine barren, forest, marshy meadow, alpine shrub and alpine meadow) in a small catchment in Qilian Mountains, northwestern China. A typical characteristic of soil in mountainous areas is widespread presence of rock and gravel, and the results showed that the more rock and gravel in the soil, the higher K_s and bulk density and the lower the soil capillary porosity, field water capacity and total

porosity. The K_s of the lower layer with rock and gravel ($18.49 \pm 10.22 \text{ mm}\cdot\text{min}^{-1}$) was significantly higher than that of the upper layer with relatively fine textured soil ($0.18 \pm 0.18 \text{ mm}\cdot\text{min}^{-1}$). The order of values of the K_s in different land cover types was alpine barren, forest, alpine shrub, marshy meadow and alpine meadow, and the values of the K_s in the alpine barren were significantly higher than those of other land covers. Most rainfall events in the research catchment had low rain intensity ($<0.04 \text{ mm}\cdot\text{min}^{-1}$), and deep percolation (DP) was the dominant runoff generation type. When the rainfall intensity increased ($0.11 \text{ mm}\cdot\text{min}^{-1}$), subsurface stormflow (SSF) appeared in the alpine meadow. Infiltration excess overland flow (IOF), SSF and DP existed simultaneously only when the rainfall intensity was extremely high ($1.91 \text{ mm}\cdot\text{min}^{-1}$). IOF and SSF were almost never appeared in the alpine barren because of high K_s . The alpine barren was the main runoff-contributed area in the mountainous catchment because of high K_s and low water-holding capacity, and the alpine shrub and meadow showed more ecological functions such as natural water storage and replenishment pool than contribution of runoff.

Received: 09-Jun-2020

Revised: 18-Aug-2020

Accepted: 10-Oct-2020

Keywords: Saturated hydraulic conductivity; Rock fragment; Land cover; Runoff generation; Mountain catchment

Introduction

Hydrological processes and the water cycle in mountainous regions are gaining increasing attention from scientists and from society (Wohl 2013), because mountainous regions are important sources of freshwater and the hydrological balance and possible future changes in mountainous regions under climate changing remain poorly understood (Dettinger 2014; Mountain Research Initiative EDW Working Group 2015; Rogora et al. 2018). The Qilian Mountains, located on the northeast margin of the Tibetan Plateau, the intersection of the Tibetan Plateau, the Mongolia Plateau and the Loess Plateau, serve as an important water source region for the Tibetan Plateau and China's northwestern inland desert region (Song et al. 2011). Towards the east of the Qilian Mountains, the Datong River flows into the Yellow River, the second largest river system in China. Many inland rivers including the Heihe River, Shule River and Shiyang River originate from the northeast of the Qilian Mountains, and provide valuable water resources for middle and lower arid regions.

Through the joint efforts of several generations of hydrologists, the generation mechanisms of rainfall and snowmelt water to surface runoff can be broadly classified into the following types: (1) infiltration excess overland flow (IOF) (Horton 1933); (2) saturation excess overland flow (SOF) (Dunne and Black 1970); (3) subsurface stormflow (SSF) (Hursh and Brater 1941); and (4) vertical flow or deep percolation (DP, water percolated through the soil profile) (Scherrer and Naef 2003). The rainfall intensity and K_s are the two most important parameters for determining type of runoff generation (Ghimire et al. 2014; Tian et al. 2017). For example, when the rainfall rate exceeds the soil infiltration capacity, water begins to fill small depressions on the landscape, resulting in a sheet of overland flow down the hillslope. This runoff generation process is defined as IOF. K_s also controls soil moisture storage and water movement, soil erosion and other land-surface processes, and

it is therefore one of the principal parameters to research for watershed hydrology, land surface-atmosphere dynamics and environmental modelling (Pan et al. 2017; Becker et al. 2018; Trinh et al. 2018).

It is well known that soil hydraulic conductivity is spatially variable, with both horizontal and vertical scales (Schwen et al. 2014), and it is more complex in high mountainous regions. One reason for the complexity is different land cover types, which leads to significant difference in soil hydraulic conductivity (Baiaomonte et al. 2017; Trinh et al. 2018). Relative to plains areas, mountainous regions have numerous different land cover types even in a very small range because of vertical zonality. For example, in the Qilian Mountains, the land cover includes glacier, alpine barren, marshy meadow, alpine meadow, alpine shrubs, forest, alpine grassland, alpine desert and cropland (Chen et al. 2018). This heterogeneity of soil hydraulic conductivity results in the unique runoff generation processes in different land cover types (Mohanty 2013). Another complexity of soil hydraulic conductivity is greater vertical variability in the high mountainous regions at soil the profile scale (Bockgård and Niemi 2004; Fu et al. 2015). Soil containing a significant fraction of gravel fragments, a notable characteristic of mountainous regions, strongly influences soil hydraulic conductivity, and increases the complexity of soil hydraulic conductivity and hydrological processes in mountainous areas (Hlaváčiková and Novák 2014). In addition, undisturbed soil sampling in gravelly and rocky soil is problematic, which makes it difficult to measure K_s in undisturbed soil. The most common way of soil sampling is by driving a cylinder into the ground, which in the case of gravelly soil may cause the displacement of rock fragments or destruction and compaction of channels present in the soil, thus leading to errors during measurements (Chappell and Lancaster 2007; Ilek and Kucza 2014). And some researchers suggested the excavation and volume determination method was more suitable to determine the bulk density of soil with high rock fragments (Page-Dumroese et al. 1999).

Although soil saturated hydraulic conductivity is a very important parameter for hydrological and other land-surface processes, it is poorly

understood because of the difficulties of obtaining measurement data in high and cold mountainous area (Ilek and Kucza 2014; Tian et al. 2017), where fieldwork is time-consuming and extremely labour-intensive (Pan et al. 2017). Due to the difficulty of field measurement and sampling, most studies focused on the horizontal variation of surface and subsurface soil hydraulic conductivity (Ghimire et al. 2014), while deeper soil and vertical variability have received very little attention (Fu et al. 2015; Tian et al. 2017). In addition, studies on soil hydraulic conductivity in high mountainous areas have mostly been conducted in forest and grassland areas at lower elevations (e.g. Ghimire et al. 2013; Pirastru et al. 2013; Ghimire et al. 2014; Zhi et al. 2017). Studies on other land cover types are few, especially on alpine barren between glacier and plant zone, referring to the high-elevation zone where little or no soil and vegetation (Hayashi 2019). Alpine barren is mainly covered by coarse sediments, such as talus, moraine, and rock glacier, and widespread at high elevation in mountainous

regions (Ruiz-Fernández et al. 2017; Hayashi 2019).

The objectives of this study were to (1) investigate soil hydraulic conductivity, (2) analyze soil hydraulic conductivity in various land cover type, and (3) characterizing runoff generation processes in a small mountainous catchment in the Qilian Mountains, northwestern China.

1 Materials and Methods

1.1 Study area

Field sampling was conducted in the Hulu catchment (99°49'E ~ 99°54'E, 38°12'N ~ 38°17'N, 2960 m~4800 m a.s.l., a drainage area of 23.1 km²), in the Qilian Mountains, northwestern China. Nearly all typical underlying surfaces can be found in the Qilian Mountains, such as glacier, alpine barren, marshy meadow, alpine meadow, alpine shrub, valley shrub, and forest (Figure 1, Table 1). Marshy meadow is wetland in high-mountain, and

alpine meadow is high-mountain meadows with low grasses. A cryosphere-hydrology observation system was established in the Hulu catchment (Chen et al. 2014). Meteorological elements such as air temperature, precipitation and multiple layers of soil water content and temperature were collected half-hourly by two automatic meteorological towers with different elevations in the Hulu catchment, which were installed in 2008 (Figure 1). The meteorological tower at the alpine meadow, location near the soil profile NO. 23 and 24, added precipitation records with finer time resolution (per minute) since March 2017. According to data from the meteorological towers, the catchment has a continental semi-arid climate characterised by warm, rainy summers and cold, dry winters. The Hulu catchment has an annual mean air

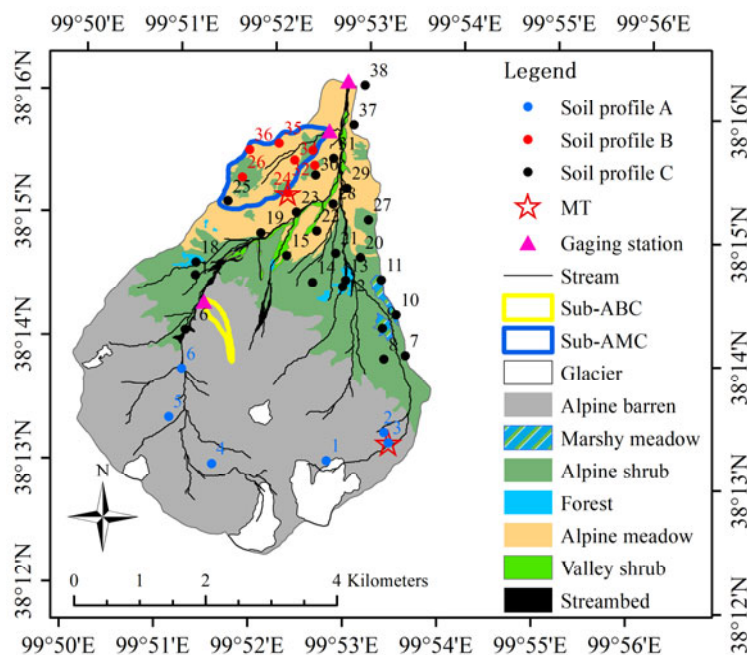


Figure 1 The map of soil profiles and hydrometeorological observation stations in the Hulu catchment (MT, meteorological tower; Sub-AMC, sub-catchment covered by alpine meadow and shrub; Sub-ABC, sub-catchment covered by alpine barren).

Table 1 The area percentages of different land covers and the number of soil profiles in the Hulu catchment

Land cover	Glacier	Alpine barren	Forest	Marshy meadow	Alpine shrub	Alpine meadow	Valley shrub	Streambed
Area percentage (%)	5.58	53.59	0.65	0.60	22.73	14.19	1.36	1.30
Soil profile	0	6	3	3	12	14	0	0

temperature of -0.3°C , and annual average precipitation of 599.8 mm. Precipitation is mainly concentrated in the wet season, which accounts for 80%~93% of annual precipitation (Han et al. 2018).

There are three stream-gauging stations in the Hulu catchment to measure runoff discharges. One station was built to monitor the total discharge at the catchment outlet. The other two stations were built for sub-catchments, one of which was covered by alpine shrub and meadow (3070 m~3580 m a.s.l, a drainage area of 1.1 km², called AMC), and one of which was covered by alpine barren (3620 m~4240 m a.s.l, a drainage area of 0.1 km², called ABC) (Figure 1). The mean annual discharge of the Hulu catchment is $0.36\text{ m}^3\cdot\text{s}^{-1}$. There are no runoff in the AMC and ABC sub-catchments during the cold months, and during the measurements, the mean discharges of AMC and ABC sub-catchments were $0.006\text{ m}^3\cdot\text{s}^{-1}$ (from March to November) and $0.005\text{ m}^3\cdot\text{s}^{-1}$ (from June to October), respectively.

1.2 Field sampling

In the summer of 2014, 38 representative soil profiles were selected for the collection of soil samples in different land cover types. These soil profiles were covered by alpine barren, marshy meadow, forest, alpine shrub and alpine meadow, which are the main land cover types in the Hulu catchment and Qilian Mountains (Figure 1, Table 1). Alpine shrub, alpine meadow and alpine barren account for more than 90% of the total area in Hulu catchment. In the alpine shrub and alpine meadow, typical soil profiles were chosen from different topographical locations (upslope, downslope, and depression). Due to the high elevation and steep topography, field sampling convenience was the first consideration for soil profiles selection in the alpine barren, then the diversity of terrain was considered.

At each soil profile, eight layers were sampled (0-10 cm, 10-20 cm, 20-30 cm, 30-40 cm, 50-60 cm, 80-90 cm, 100-110 cm and 150-160 cm), and both disturbed and undisturbed soil samples were collected. The cylinder, a steel core sampler with a 200cm³ volume (7 cm diameter and 5.2 cm height), was slowly pushed vertically at the top of each layer to collect the undisturbed soil core for each layer. In order to avoid the disturbance, every cylinder was inserted into the soils carefully. The

cylinders were sealed and protected by plastic shields before taken to the laboratory. Three duplicate undisturbed samples were collected at each layer. The disturbed soils were collected from the entire soil horizon with a shovel, the same locations where the cylinder sampled. The disturbed soil samples were collected into cloth bags carefully. It should be noted that some soil profiles covered by alpine barren and marshy meadow at high elevation only had the first five layers (0-50 cm depth) or six five layers (0-80 cm depth). In the alpine barren, there were large rocks in the soil, making it was impossible to dig soil profiles up to 150 cm depth and field deeper samples. The size of gravel on the deeper layer under alpine barren is too large to be sampled with cylinder, so soil samples were collected under alpine barren only had the first five layers (0-50 cm depth). In the marshy meadow, the soil was almost saturated, and there was lateral flow at the soil profiles, which quickly became water holes. In total, the number of soil sampling layers was 289 in 38 soil profiles. The number of soil profiles on different land cover types can be seen in Table 1. All of the soil samples were carefully taken to the laboratory.

1.3 Laboratory analysis

Soil in mountainous areas is characterised by high gravel content, and sometimes there is little soil with small particle sizes, but more gravel and rock (particle size $>2\text{ mm}$), as was the case with some of the some soil profiles at the alpine barren or the deeper soil layers at other land cover types. For convenience, this paper used word "soil" to describe all coverings of the land surface, includes soil, gravel and rock under the actual natural conditions. The disturbed samples were used to measure soil particle size distribution. First, the soil samples were air-dried and passed through 5 mm and 2 mm sieves, and they were then dispersed in sodium hexametaphosphate and analyzed for particle size distribution by the hydrometer method (Gee and Bauder 1986). In line with U.S. Department of Agriculture classification standards, the soil with small particle sizes ($<2\text{ mm}$) was classified as sand (0.05 mm~2 mm), silt (0.002~0.05 mm) and clay ($<0.002\text{ mm}$). The soil textures in this study were classified as rock (>5

mm), gravel (2~5 mm), sand, silt and clay.

The undisturbed samples were used to determine the soils physical and hydraulic properties including soil capillary porosity (CP, %), total porosity (TP, %), field water capacity (FC, %), bulk density (BD, g·cm⁻³) and saturated hydraulic conductivity (K_s , mm·min⁻¹). The collected samples were first wetted 5 mm deep with water for 8 hours and weighed (W_1) to measure CP. Second, the cores were soaked in 5 cm depth water for approximately 24 hours until saturated, and the samples were weighed (W_2) to measure TP. Third weight, W_3 was recorded to measure FC after the soil samples were put on dry sand for 24 hours. Fourth, the constant hydraulic head method was used to determine K_s . To prevent disturbance of the soil surface, a filter paper was put on top of each core, and an empty cylinder with the same size was tightly secured to act as a reservoir, and cylinder cores were linked to a Mariotte's bottle and supplied with water from the top. The Mariotte's bottle was used to keep a constant head (3 cm), and the mass of water eluted from the sample cylinder was measured when flux rate became steady. The temperature (T , °C) during the experiment was recorded using a thermometer. Finally, the cores were oven dried at 105°C for 24 hours and weighed (W_4). No perceivable swelling was detected in any of the cores during the soaking process. The soil physical and hydraulic properties were calculated using the following formulas (Fu et al. 2015; Pan et al. 2017):

$$CP = (W_1 - W_4) / (\rho V) \times 100\% \quad (1)$$

$$TP = (W_2 - W_4) / (\rho V) \times 100\% \quad (2)$$

$$FC = (W_3 - W_4) / (\rho V) \times 100\% \quad (3)$$

$$BD = (W_4 - W_0) / V \quad (4)$$

$$K_{s,T} = 10QL / (A \times \Delta h \times t) \quad (5)$$

$$K_s = K_{s,T} / (0.7 + 0.03 \times T) \quad (6)$$

where, ρ is water density (1 g·cm⁻³), W_{1-4} is the weights of the cylinder cores with soil samples in the experiment procedure (g), W_0 is the weights of the cylinder cores without soil (g), V is the volume of the cylinder cores (200 cm³), $K_{s,T}$ is the saturated hydraulic conductivity at experiment temperature (T , °C)(mm·min⁻¹), K_s is the saturated hydraulic conductivity at 10°C (mm·min⁻¹), Q is the water volume (cm³), L is the length of the soil core (5.2 cm), A is the cross-sectional area of the soil core

(38.46 cm²), t is the time (min) and Δh is the height difference of the hydraulic head (3 cm).

1.4 Rainfall intensity measurement

The vertical distribution of K_s and rainfall intensity are the most important parameters governing runoff generation types during and shortly after rainfall events (Zimmermann and Elsenbeer 2009; Ghimire et al. 2014). The runoff generation type can be interpreted to reveal the proportion of IOF, SSF and DP in response to rainfall, by superimposing maximum rainfall intensity on K_s of different layers (Zimmermann et al. 2006; Ghimire et al. 2014; Tian et al. 2017). Rainfall intensities were collected by the automatic meteorological towers at the alpine meadow in the Hulu catchment (Figure 1). With reference to research on other regions (Zimmermann and Elsenbeer 2009; Ghimire et al. 2014), the lower quartile, median, upper quartile, 95th percentile and maximum values were selected as indices for inferring the dominant runoff generation type during rainfall.

1.5 Statistical analysis

The classical statistics of the maximum, minimum, mean, standard deviation (SD), and coefficient of variation (CV) were obtained for the soil properties. Pearson's correlation coefficient was used to determine the relationships between the soil properties. All analyses were performed using SPSS software version 20.0 (IBM, Armonk, NY, USA).

2 Results

2.1 Vertical distributions of soil properties

Vertical variations in soil hydraulic properties were significantly associated with soil horizons. The vertical variability of soil hydraulic properties in the clear duplex soil profile (texture-contrast) was obviously greater than the variability in the uniform soil profiles. There were three typical vertical soil profiles in the research catchment. The first type included all six soil profiles at the alpine barren, which were homogeneous vertically with a

great deal of rocks and gravels (soil profile A in Figure 1). For example, profile NO.4 (Figure 2a, Figure 3a), had rocks and gravel in each layer, and the maximum, minimum and mean of the rock content were 58.32%, 46.82% and 52.95%, respectively. Rocks and gravel with the particle sizes larger than 2 mm were the main components of each layer (Figure 3a, Table 2). Because of the formation of macropores from the rocks and gravel, the K_s values in the profile were relatively high: the maximum and minimum of the K_s in the five layers (0-50 cm) were 37.91 mm·min⁻¹ and 22.20 mm·min⁻¹, respectively, and the mean K_s was 30.19 mm·min⁻¹. The CV of the K_s in the profile was small, with value of 0.19, which meant that the K_s varied little at different depths. The CV of other soil

physical and hydraulic properties, such as BD, CP, FC and TP, showed that they also varied little at different depths (Table 2). The CP, FC and TP did not show significant change trends in the vertical direction, while the K_s and BD increased with depth.

The second type included soil profiles from the alpine meadow (NO. 24, 34, 35 and 36) and alpine shrub (NO. 26, 32 and 33) areas, which were homogeneous vertically at 150 cm depth with little rocks and gravel distribution (soil profile B in Figure 1). For example, in the profile NO.35, there were no rocks and little gravel in the soil profile, and the mean of the gravel content was 0.72% (Figure 3e, Table 2). The maximum, minimum and mean of the K_s at all eight layers in this profile were

0.19 mm·min⁻¹, 0.06 mm·min⁻¹ and 0.11 mm·min⁻¹, respectively. As the soil depth deepened, the K_s gradually decreased, and then increased below 80 cm depth (Figure 2e). The CP, FC and TP increased with depth, reaching maximum at 50 cm, and then began to decrease. The BD showed a slight increasing trend as the depth increased. Because there was no clear gravel and rocks layer in these soil profiles with 150 cm depth, the CV of the soil physical and hydraulic properties were relative small, and were particularly smaller than the third type of soil profile.

The third type of soil profile featured an upper layer of soil with no or less rock and gravel, and a lower layer with clear rocks and gravel (soil profile C in Figure 1). The first type included 6 profiles, the second included 7 profiles, and the third type included 25 profiles. Profile NO.10

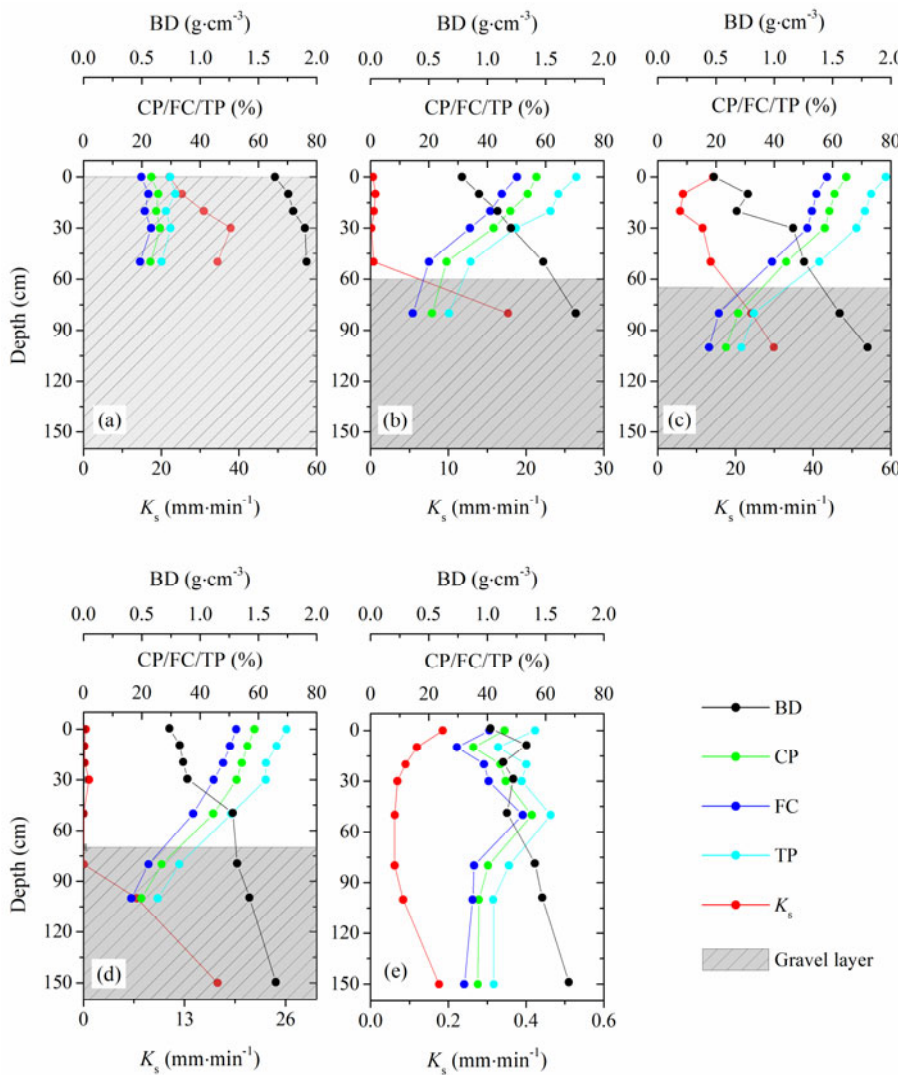


Figure 2 Soil saturated hydraulic conductivity (K_s), bulk density (BD), soil capillary porosity (CP), field water capacity (FC) and total porosity (TP) for soil profile NO.4 (a), NO.10 (b), NO.12 (c), NO.17 (d) and NO.35 (e) in the Hulu catchment.

at marshy meadow (Figure 2b, Figure 3b), profile NO.12 at forest land cover (Figure 2c, Figure 3c) and profile NO.17 at alpine shrub (Figure 2d, Figure 3d) were chosen to illustrate the vertical variability of the soil physical and hydraulic properties. It was very clear that the soil with large particle size, especially rock content, increased sharply in the deeper soil, and the rock content in deeper soil layers was much larger than in the layers (Figure 3b, 3c and 3d). Because of the significant variation in the soil physical and hydraulic properties between soil layers with or without rocks and gravels, the K_s , BD, CP, FC and TP in the upper and lower layers showed significant differences. The means \pm SD of the K_s for the lower layer with rock and gravel from 22 profiles at marshy meadow, alpine meadow and alpine shrub was $18.49 \pm 10.22 \text{ mm}\cdot\text{min}^{-1}$, and $0.18 \pm 0.18 \text{ mm}\cdot\text{min}^{-1}$ for the upper layer with relatively

fine textured soil. The vertical variation of K_s in uniform fine textured or rock and gravel layer is much less than the variation in the clear duplex soil profile, and the CV of the K_s for the upper layer, lower layer and the profiles were 1.00, 0.55 and 1.57, respectively. The CP, FC and TP decreased as depth increased, while the K_s and BD increased. The larger CV of K_s , BD, CP, FC and TP showed that the vertical variability of soil physical and hydraulic properties in these profiles were much more significant than those of the former two types (Table 2). The K_s showed the most dramatic change: the ratios of the maximum and minimum K_s for profiles NO.10 and NO.17 were 63 and 36, respectively. The K_s at the upper layers in the profile NO.12 were not as small as those in profiles NO.10 and NO.17, and the vertical variability of the K_s at this profile was not as sharp as those of the other two profiles. This profile was forest land

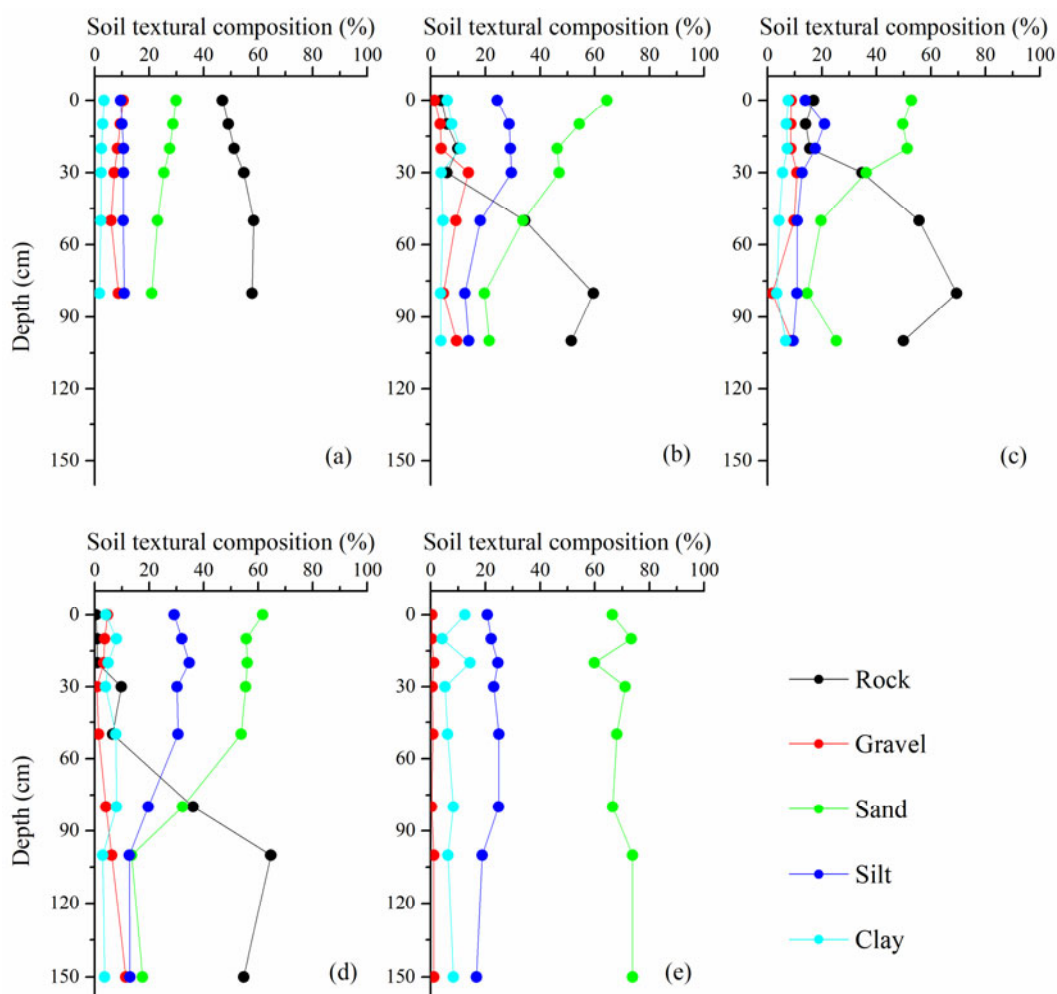


Figure 3 Soil textural composition for soil profiles NO.4 (a), NO.10 (b), NO.12 (c), NO.17 (d) and NO.35 (e) in the Hulu catchment.

Table 2 Maximum, minimum, mean, standard deviation (SD) and coefficient of variation (CV) of soil properties of the soil layers for different soil profiles in the Hulu catchment.

Soil profiles	Land covers	Statistics	K_s (mm·min ⁻¹)	BD (g·cm ⁻³)	CP (%)	FC (%)	TP (%)	Rock (%)	Gravel (%)
NO.4	Alpine barren	Maximum	37.91	1.91	26.32	23.20	31.55	58.32	10.50
		Minimum	22.20	1.64	22.99	19.42	26.79	46.82	5.95
		Mean	30.19	1.80	24.65	21.16	29.25	52.95	8.34
		SD	5.77	0.10	1.30	1.43	1.60	4.32	1.48
		CV	0.19	0.06	0.05	0.07	0.05	0.08	0.18
NO.10	Marshy meadow	Maximum	17.68	1.76	56.96	50.27	70.61	59.53	13.76
		Minimum	0.11	0.78	21.12	14.53	26.99	3.84	1.33
		Mean	3.26	1.21	41.38	34.18	51.33	24.45	6.52
		SD	6.45	0.33	13.46	12.98	15.99	21.97	4.07
		CV	1.98	0.27	0.33	0.38	0.31	0.90	0.62
NO.12	Forest	Maximum	29.89	1.80	64.71	58.14	78.27	69.38	10.82
		Minimum	5.79	0.48	23.43	17.64	28.75	13.94	1.77
		Mean	15.13	1.10	48.11	42.10	58.32	36.55	8.13
		SD	8.24	0.45	15.48	15.43	18.53	20.56	2.71
		CV	0.54	0.41	0.32	0.37	0.32	0.56	0.33
NO.17	Alpine shrub	Maximum	17.28	1.65	58.69	52.41	69.70	64.61	11.31
		Minimum	0.03	0.74	19.90	16.40	25.50	0.47	0.79
		Mean	3.19	1.12	44.73	38.80	52.89	21.74	4.42
		SD	5.76	0.31	14.22	13.15	16.05	24.56	3.07
		CV	1.80	0.28	0.32	0.34	0.30	1.13	0.69
NO.35	Alpine meadow	Maximum	0.19	1.70	55.34	52.22	61.78	0.00	1.17
		Minimum	0.06	1.03	35.31	29.62	42.12	0.00	0.30
		Mean	0.11	1.31	42.74	38.10	49.89	0.00	0.72
		SD	0.05	0.20	6.26	6.48	6.73	0.00	0.35
		CV	0.44	0.15	0.15	0.17	0.13	0.00	0.49

Note: K_s , soil saturated hydraulic conductivity; BD, bulk density; CP, soil capillary porosity; FC, field water capacity; TP, total porosity; Rock, rock content; Gravel, gravel content.

cover, and the greater amounts of organic matter and humus in the forest increased the K_s (Pirastru et al. 2013; Ghimire et al. 2014).

2.2 Variability of soil properties in different land cover types

The vertical variability of soil properties was introduced in the previous section, and runoff generation types were mainly related to the soil surface K_s , so only the soil properties at surface layer for the different land covers are discussed in this section.

The effects of land cover on the K_s and other soil physical and hydraulic properties at surface layer are shown in Figure 4. The mean values of the K_s for different land covers were in the order of alpine barren > forest > alpine shrub > marshy meadow > alpine meadow (Figure 4a). The means \pm SD of the K_s for alpine barren, marshy meadow, forest, alpine shrub and alpine meadow were 17.02 ± 8.75 mm·min⁻¹, 0.37 ± 0.14 mm·min⁻¹, 11.07 ± 4.29 mm·min⁻¹, 0.71 ± 0.87 mm·min⁻¹ and $0.15 \pm$

0.07 mm·min⁻¹, respectively. The values of the K_s in the alpine barren were significantly higher than those of other land covers, particularly alpine meadow, and the mean values of the K_s of the alpine barren was about 113 times that of alpine meadow.

The BD for the alpine barren was significantly higher than those of the other land covers, because the soil particles were coarse and the rock and gravel content was higher than those of other land covers (Figure 4f, 4g), with the sum of rock and gravel content over 50%. The soil profiles at the forest land cover had the lowest BD at surface layer (Figure 4b) because of the high amount of organic matter. There was no significant difference in surface BD for marshy meadow, alpine shrub and alpine meadow, and the means \pm SD of BD were 0.74 ± 0.09 g·cm⁻³, 0.74 ± 0.13 g·cm⁻³ and 0.77 ± 0.16 g·cm⁻³, respectively.

The CP, FC and TP for different land covers showed similar variability (Figure 4c, 4d, 4e). On the whole, the CP, FC and TP for the alpine barren were significantly lower than those of the plant

land covers. For all of the plant land covers, the soil surface at the alpine meadow had the lowest CP, FC and TP, and the soil surface at the forest had the highest CP, FC and TP.

The large particle size content in the soil was also related to the type of land cover. The rock and gravel content in the soil surface for the different land covers was in the order of alpine barren > forest > alpine shrub > marshy meadow > alpine meadow (Figure 4f, 4g). There was almost no rock in the surface soil in the alpine meadow land cover, and the mean \pm SD value of rock content was 0.72 ± 0.36 % from all 14 soil profiles. Relatively lower rock and gravel contents might be the reason for that the surface K_s in the marshy meadow, alpine shrub and alpine meadow were significantly lower than those of other land covers.

2.3 Relationships between K_s and soil properties

Pearson correlation coefficients used to analyze the soil properties (Table 3) revealed that K_s was positively correlated with BD, rock and gravel content but negatively correlated with CP, FC, TP, sand content, silt content and clay content. The correlation between K_s and the other soil properties possibly because large-grained particle like rock and gravel was ubiquitous in the Hulu catchment, leading to apparent higher K_s , higher BD and lower CP, FC and TP. BD was positively

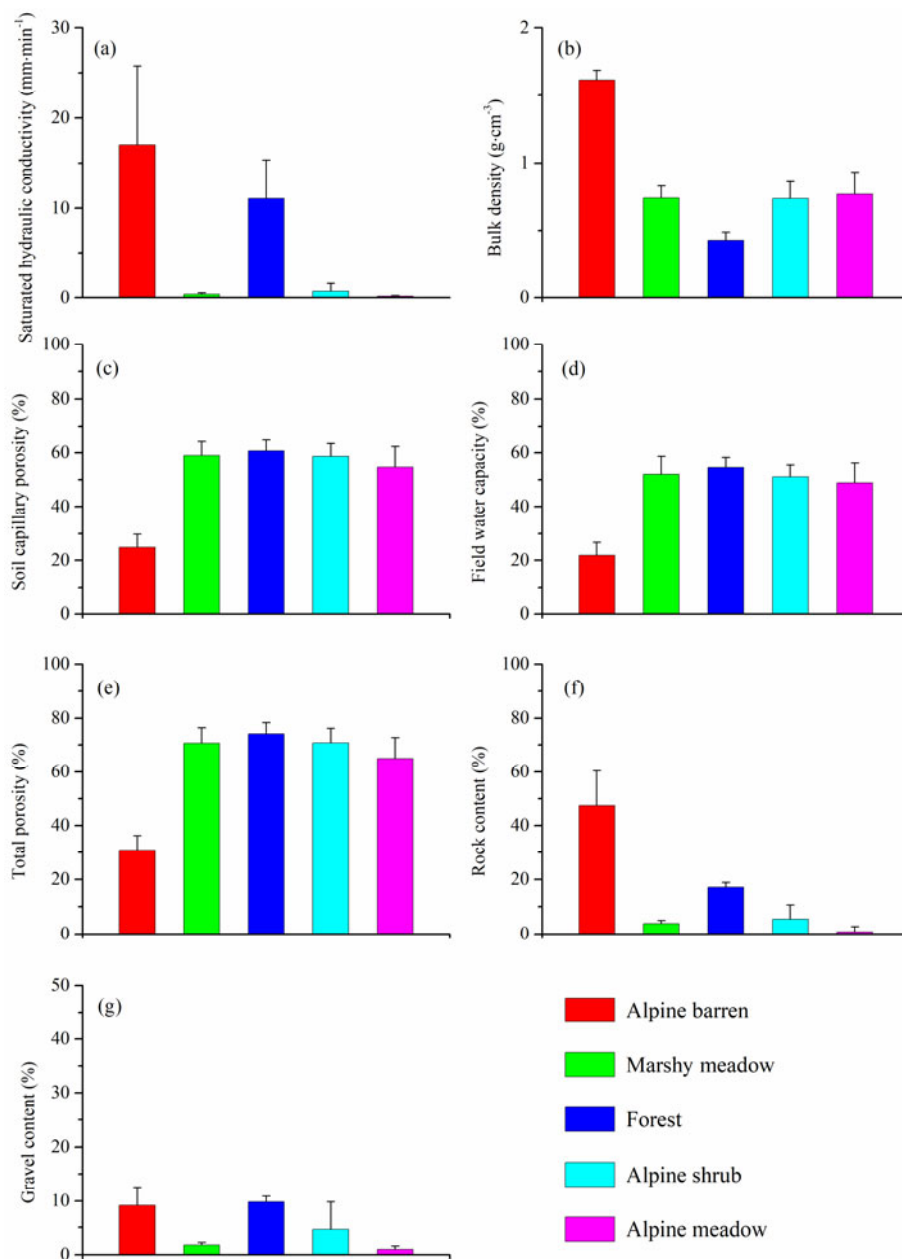


Figure 4 Differences in soil saturated hydraulic conductivity (a), bulk density (b), soil capillary porosity (c), field water capacity (d), total porosity (e), rock content (f) and gravel content (g) at soil surface layer in different land cover types.

correlated with rock and gravel content but negatively correlated with CP, FC, TP, sand content, silt content and clay content. As mentioned in previous sections, the variation trends of CP, FC and TP were similar, and the correlation coefficients of CP, FC and TP all above 0.97. CP, FC and TP were negatively correlated with rock and gravel content but positively correlated with sand content, silt content and clay content. Rock content was positively correlated with gravel content, and

Table 3 Pearson correlation coefficients between K_s (saturated hydraulic conductivity, $\text{mm}\cdot\text{min}^{-1}$), BD (bulk density, $\text{g}\cdot\text{cm}^{-3}$), CP (capillary porosity, %), FC (field water capacity, %), TP (total porosity, %) and the soil texture content (%) in the research watershed

	K_s	BD	CP	FC	TP	Rock	Gravel	Sand	Silt	Clay
K_s	1									
BD	0.558**	1								
CP	-0.578**	-0.888**	1							
FC	-0.548**	-0.872**	0.992**	1						
TP	-0.574**	-0.907**	0.990**	0.977**	1					
Rock	0.809**	0.544**	-0.588**	-0.570**	-0.565**	1				
Gravel	0.212**	0.166*	-0.193**	-0.195**	-0.181**	0.256**	1			
Sand	-0.704**	-0.452**	0.487**	0.476**	0.469**	-0.919**	-0.495**	1		
Silt	-0.662**	-0.521**	0.579**	0.556**	0.553**	-0.701**	-0.368**	0.525**	1	
Clay	-0.416**	-0.269**	0.296**	0.287**	0.276**	-0.504**	-0.201**	0.415**	0.226**	1

Note: ** significant at the 0.01 level; * significant at the 0.05 level (two-tailed test); $n=220$.

both were negatively correlated with sand content, silt content and clay content. Sand content, silt content and clay content were positively correlated with each other.

2.4 Rainfall intensity and runoff generation types

A total of 20,387 rainfall events were recorded during the warm seasons (May to September) of 2017 and 2018 at the automatic meteorological tower near the AMC (Figure 1). During the study period, the mean monthly precipitation was 88.0 mm and the maximum rainfall amount was 24.4 mm, from 6:11 to 14:23 on July 18, 2018. The longest rainfall duration was from 20:52 on June 3, to 5:42 on June 4, 2017, with an amount of 8.8 mm. The maximum minute intensity for rainfall events over the two monsoon seasons was $1.91 \text{ mm}\cdot\text{min}^{-1}$, and the lower quartile, median, upper quartile and 95th percentile were $0.01 \text{ mm}\cdot\text{min}^{-1}$, $0.02 \text{ mm}\cdot\text{min}^{-1}$, $0.04 \text{ mm}\cdot\text{min}^{-1}$ and $0.11 \text{ mm}\cdot\text{min}^{-1}$, respectively (Figure 5). In the research region, considerably more than half of all rainfall events had a maximum intensity of $0.04 \text{ mm}\cdot\text{min}^{-1}$; greater intensities occurred much less frequently. The greatest portion of the total rain amount (58%), however, is associated with rain intensities exceeding the upper quartile amounting to $0.04 \text{ mm}\cdot\text{min}^{-1}$. Rainfall events with an intensity of more than $0.11 \text{ mm}\cdot\text{min}^{-1}$ accounted for only 4.4% of the total events, but the precipitation accounted for 21.55% of the total precipitation.

Following other hydrologists' research methods (Zimmermann and Elsenbeer 2009; Ghimire et al. 2014), the lower quartile, median,

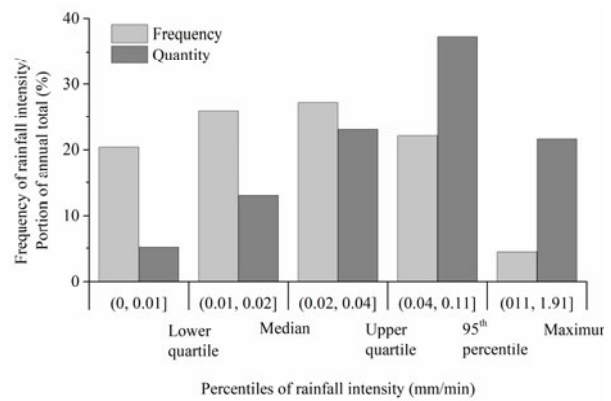


Figure 5 Frequency and quantity of rainfall intensities as recorded at the automatic meteorological tower in the Hulu catchment during the 2017 and 2018 warm seasons (May to September).

upper quartile, 95th percentile and maximum value of rainfall intensity were selected as indices for inferring the dominant runoff generation types. These have been plotted in conjunction with the results obtained for the K_s for the respective land covers in Figure 6. When the rainfall intensity exceeded the surface K_s , IOF occurred. When vertical water flow from upper layer exceeded the K_s in the soil layer, SSF occurred. DP is permeable water flow to the bottom of the soil profile.

For the alpine barren (Figure 6a) and forest (Figure 6e), the maximum rainfall intensities were much lower than the K_s at different depths, IOF and SSF were not found, and DP was the inferred dominant runoff generation type. The upper quartiles of rainfall intensities for other three land cover types were lower than the K_s at different depths, indicating that DP was the inferred dominant runoff generation type for all rainfall events with these intensities (Figure 6b, 6c, 6d). However, when the rainfall intensity exceeded 0.04

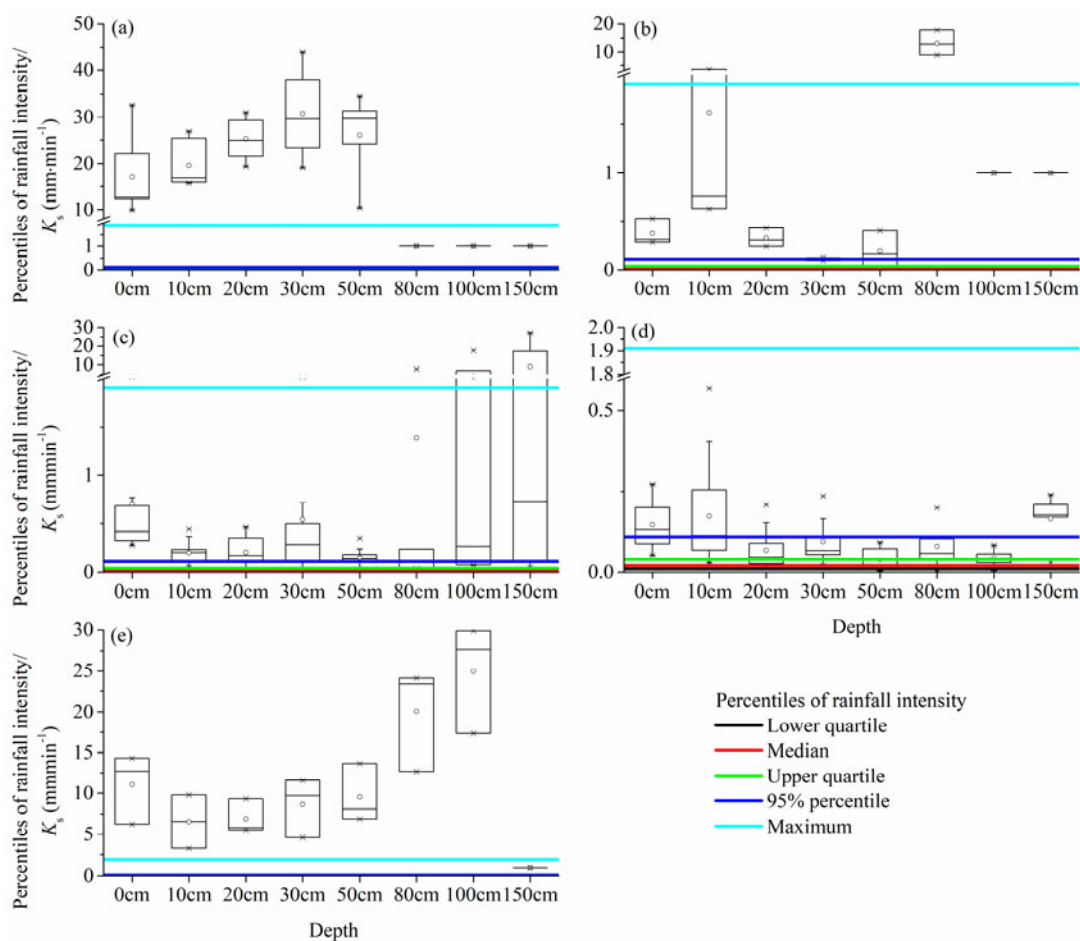


Figure 6 Box plots of soil saturated hydraulic conductivity (K_s) for alpine barren (a), marshy meadow (b), alpine shrub (c), alpine meadow (d) and forest (e) at different depths. The solid horizontal lines represent percentiles of rainfall intensity.

$\text{mm}\cdot\text{min}^{-1}$ (upper quartiles) and reached $0.11 \text{ mm}\cdot\text{min}^{-1}$ (95% percentile), the rainfall intensity was higher than the K_s at 20 cm and 30 cm depths for alpine meadow (Figure 6d). Thus, as another runoff generation type, SSF would appear. In the precipitation intensity interval from $0.04 \text{ mm}\cdot\text{min}^{-1}$ to $0.11 \text{ mm}\cdot\text{min}^{-1}$, DP still was the dominant runoff generation type for marshy meadow and alpine shrub. The rainfall intensity was further increased to the maximum of $1.91 \text{ mm}\cdot\text{min}^{-1}$, which exceeded the K_s at the soil surface in the marshy meadow, alpine shrub and alpine meadow (Figure 6b, 6c, 6d). Thus, IOF became the dominant runoff generation type, and various forms of runoff generation existed simultaneously.

By comparing the rainfall intensity with the vertical distribution of K_s , soil hydrological processes and runoff generation types can be analyzed during storm events (Ghimire et al. 2014, Tian et al. 2017). Figure 7 shows the percentages of

different runoff generation types under different land covers at the maximum intensity of $1.91 \text{ mm}\cdot\text{min}^{-1}$. IOF, SSF and DP existed simultaneously under the marshy meadow, alpine shrub and alpine meadow, and IOF accounted for the largest proportion of runoff generation, following SSF and DP. No IOF or SSF was found in the alpine barren and forest because of the high K_s , and DP was the only runoff generation type in those two land covers.

3 Discussion

3.1 Influence of large-grained rock and gravel on K_s

Soil containing rock and gravel is common in high mountainous areas (Hlaváčiková et al. 2019), and the influence of large-grained rock fragments on K_s is significant and inconsistent (Zhang et al.

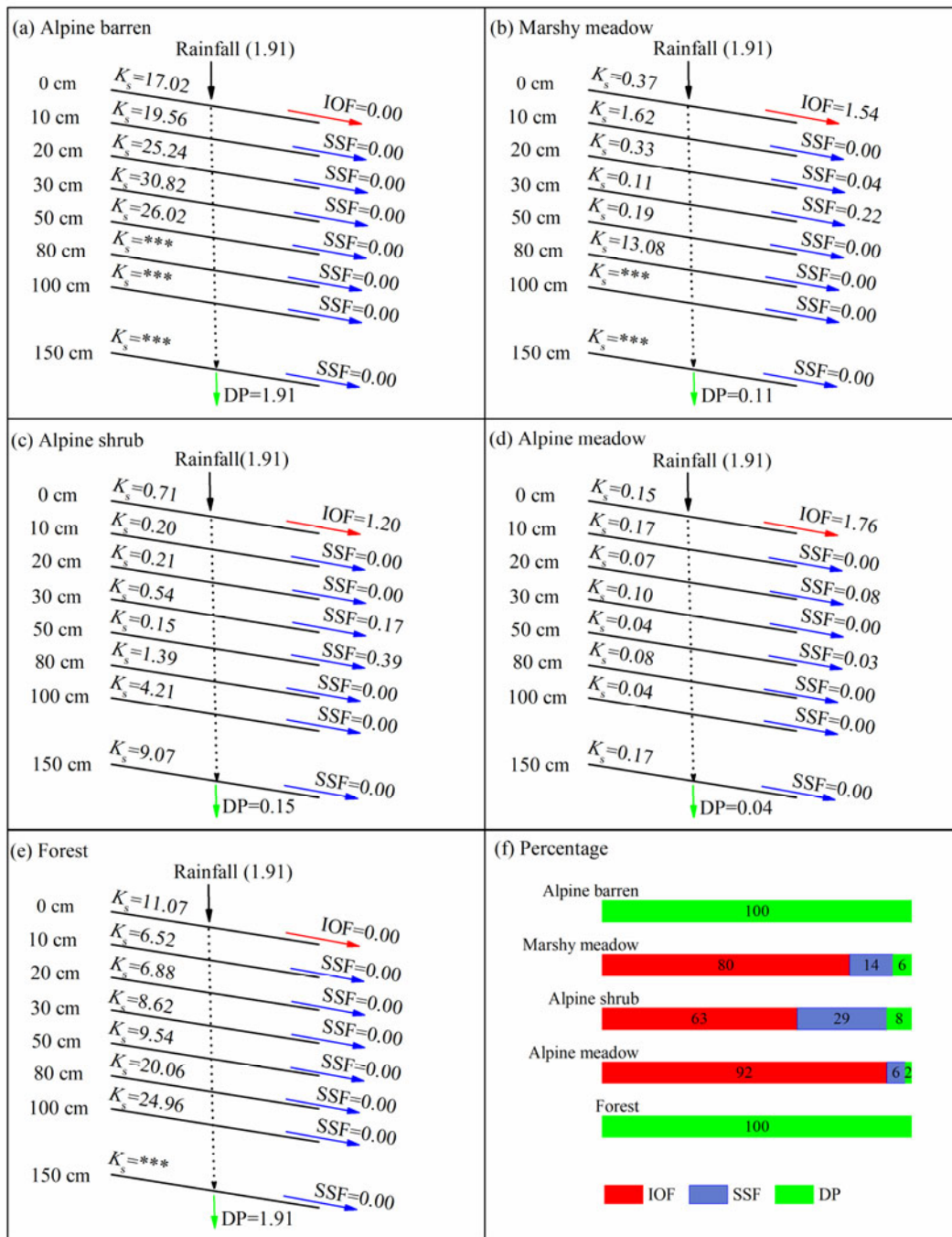


Figure 7 The percolation of rainfall delivered at the maximum intensity of $1.91 \text{ mm}\cdot\text{min}^{-1}$ through various soil layers for contrasting land covers in the Hulu catchment. IOF is the infiltration excess overland flow, SSF is the subsurface flow and DP is the deep percolation. The unit of rainfall intensity, K_s (soil saturated hydraulic conductivity) and the rate of runoff generation types are $\text{mm}\cdot\text{min}^{-1}$. ***, no data.

2016). As rock fragments could reduce the pore volume available for containing water and the area available for water flow and increase the tortuosity of water flow paths, K_s generally decreased with increasing rock fragments (Baetens et al. 2009, Lai et al. 2018). Conversely, some studies showed that

rock and gravel could increase K_s , because rock fragments in soil tend to widen the effective pore-size distribution (Jomaa et al. 2012, Naseri et al. 2019). The influence of rock fragments on K_s is very complicated because many factors, including coverage, content, size, spatial heterogeneity,

position, morphology, weathering and topography of rock fragments could all affect K_s (Zhang et al. 2016).

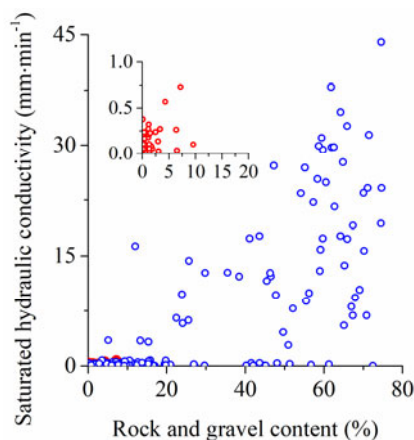


Figure 8 The relationship between saturated hydraulic conductivity and the rock and gravel content in the Hulu catchment. The red circles indicate soil samples with gravel fragment only and the blue circles indicate the soil samples with gravel and rock fragments.

Field observation and laboratory particle size analysis showed that large-grained particle like rock and gravel was ubiquitous in the Hulu catchment. Of the 289 soil sampling points from 38 soil profiles, 42 sampling points had no rock and only one sampling point had no rock and no gravel in the soil. Figure 8 shows the relationship between K_s and the rock and gravel content, and the rock and gravel were more likely to increase K_s in the Hulu catchment. In addition to rock and gravel, sand was a main component of the soil in the Hulu catchment, and coarse particles were main components of mountain soil (Figure 3). Sandy soils are generally associated with large soil pores and higher K_s than fine textured soils (Macinnis-Ng et al. 2010). The presence of rock could prevent pores from being filled with a finer material (Fiès et al. 2002) and increase the pores - especially macropores - in the soil (Hlaváčiková et al. 2019), leading to apparent higher K_s .

Another remarkable feature in the research region was a significant layer of gravel under a fine textured soil layer, which formed a clear duplex soil profile (texture-contrast) (Figure 2). Duplex soil generally presents a significant difference between the upper and lower soil layers, and in many places like farm land in Australia or oases in northwest China, the texture of the subsoil is finer than that of the surface soil, and the K_s of the upper layer is

higher (Macinnis-Ng et al. 2010; Zhou et al. 2016). This difference usually resulted in perched water tables and subsurface lateral flow in the interface (Hardie et al. 2012). However, the duplex soil in the Hulu catchment showed a completely different phenomenon: the upper layer had a finer texture and the lower layer had significantly higher K_s . When the water reaches the interface, it would quickly infiltrate down to a deeper level, making it difficult to form a soil water pool or lateral flow. In the alpine barren with high elevation above the vegetation line, rock fragments with large particles were the main component of the surface land cover, and could be treated as a complete gravel layer. The K_s of each layer in the alpine barren was larger, and rainfall would directly infiltrate quickly.

3.2 Runoff contribution in different land cover types

Alpine barren, alpine shrub and meadow account for the vast majority of land cover in the mountainous catchment (Figure 1), and the soil properties showed significant variability (Figure 4). The alpine barren had high K_s and low water-holding capacity, whereas the shrub and meadow had low K_s and high water-holding capacity. When rainfall occurred, the soil moisture in the near surface (10 cm and 20 cm depths) responded and rose rapidly both in the alpine barren and meadow. However, because of differences in soil properties, the response time of the deeper (40 cm and 60 cm depths) soil water content in the alpine barren was much shorter, and it took more time to infiltrate to deeper soil in the meadow land cover. When rainfall stopped, the soil water content decreased rapidly in the alpine barren and slowly in the meadow because of its low K_s and high water-holding capacity (Figure 9). The variability of soil properties could also affect the response of soil water content to rainfall intensity and rainfall amount. The soil water content in meadow only responded quickly to heavy rainfall, while the soil water content in alpine barren could also respond quickly to small rainfall (Figure 9).

Soil from alpine barren showed the significant differences in K_s and other soil properties to soil from alpine shrub and meadow, and the ABC covered by alpine barren also showed the differences in flood discharge hydrograph to AMC

covered by alpine shrub and meadow (Figure 10). The rainfall passed the alpine barren and entered the river quickly, and runoff was generated quickly in ABC. The flood peak formed earlier and the flood recessed quicker in the ABC than the AMC, and the runoff process in the ABC responded to rainfall more quickly and directly. In AMC, runoff was generated when soil saturation or extra water infiltrated to a deeper layer and formed DP. In this situation, some of the rainfall would be stored in the soil and released slowly. In addition, interception from the shrub and alpine meadow consumed a certain percentage of rainfall (Sun et al. 2016; Chen et al. 2018). There may be very rare cushion plants in the alpine barren, and their interception of rainfall was very weak. Because of the low soil water content and low temperature with high elevation, evapotranspiration is low in the alpine barren (Chen and Han 2010; Han et al. 2013). High K_s , low water-holding capacity, low evapotranspiration and steep terrain caused most of the rainfall that was directly generated to runoff in the alpine barren. All of these factors caused the runoff coefficients of the alpine barren to be much higher than other plant zone: the annual average runoff coefficients of the ABC and AMC were 0.72 and 0.17, respectively (Han et al. 2013; Yang 2013). With sufficient objective area distribution and a high runoff coefficient, the runoff in the mountain catchment was mainly contributed by the alpine barren. The recession curve of the discharge hydrograph of the Hulu catchment was similar to the hydrograph of the ABC (Figure 10), and it could be considered that the discharge of Hulu was more related to the runoff generation of the alpine barren. The hydrological model showed that the alpine barren region contributed 60% of the runoff, even though it made up only about 20% of the upstream Heihe area (Chen et al. 2018). As widely distributed land cover in mountainous regions, the shrub and alpine meadows might not contribute the most runoff; however, soil in those areas could

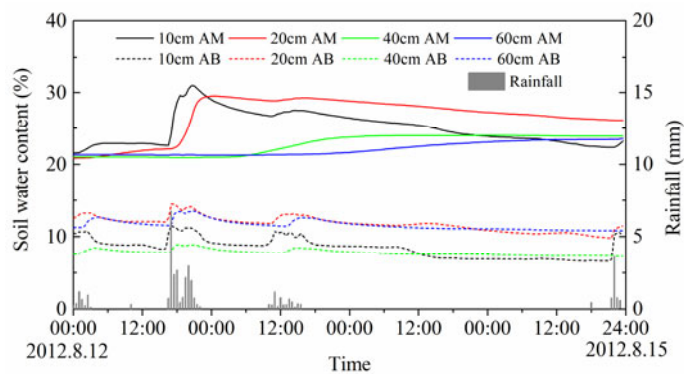


Figure 9 Soil water content at different depths in the alpine meadow (AM) and alpine barren (AB) land covers for the storm events in the Hulu catchment from 12 August to 15 August, 2012.

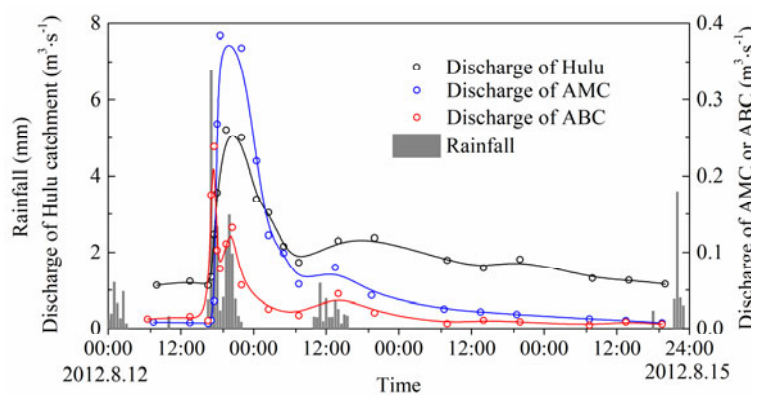


Figure 10 Discharge hydrographs for the storm events in two sub-catchments and the Hulu catchment from 12 August to 15 August, 2012. (The black, blue and red lines are B-spline curve fittings for the discharge of the Hulu catchment, AMC and ABC, respectively. AMC, sub-catchment covered by alpine meadow and shrub; ABC, sub-catchment covered by alpine barren).

provide sufficient usable water for plant growth because of low K_s and high water-holding capacity, which is essential in high elevation mountain ecosystems (Sun et al. 2015, Tian et al. 2019).

3.3 Uncertainties and implications of this study

A soil cylinder core sampling method was used to measure K_s , which was the key parameter in this study. In addition to this method, there are many other field measurement methods for obtaining K_s , such as single-ring and double-ring infiltrometers, tension permeameter, constant-head well permeameters and rainfall simulators (Jiang et al. 2017; Morbidelli et al. 2017). These methods have different systematic errors and biases and produce inconsistent and sometimes conflicting results

(Zhang and Schaap 2019). In general, the double-ring infiltrometer is considered a relatively accurate method (Fatehnia et al. 2016; Picciafuoco et al. 2019), but some reports suggested that this method could give higher K_s for soil with rock fragments (Ronayne et al. 2012; Verbist et al. 2013). Due to the complexity of the influence of large-grained rock fragments on hydraulic conductivity, a large soil sampling size might be better (Germer and Braun 2015). Because of harsh field conditions in high mountainous regions, the soil sample size in this study might not be so large, but compared with the measured results of other reports, the measured K_s and other soil properties were reasonable. The surface soil K_s value in the region near the NO.38 soil profile (Figure 1) measured by double-ring infiltrometer was $0.39 \text{ mm}\cdot\text{min}^{-1}$ (Yang et al. 2017), whereas the K_s value measured by soil cylinder core sampling in this study was $0.11 \text{ mm}\cdot\text{min}^{-1}$. Tian et al. (2017) reported that the mean surface soil K_s value measured by soil cylinder core sampling for alpine meadow in Qilian Mountains was $0.10 \text{ mm}\cdot\text{min}^{-1}$, whereas the mean K_s was $0.15 \text{ mm}\cdot\text{min}^{-1}$ in this study. High elevation mountain areas are important water source areas; however, the field sampling and experiments in this area are quite difficult because of the extremely harsh environment, roadless terrain, rock fragments complicating field measurements, etc. (Hlaváčiková et al. 2019). To the best of our knowledge, this might be the first report on K_s of different land cover types in such a small catchment in such high elevation mountains. The measured data showed great complexity and variability of the spatial and vertical K_s and other soil properties, which is of great significance for research on hydrological and other land-surface processes and hydrological models in high elevation mountain areas.

Mountains contribute a meaningful proportion of the world's freshwater supply; however, due to the high elevation, harsh environment and extremely rare observations on hydrology and water balance, hydrological processes in mountainous regions remain poorly understood, and climate change has increased the temporal and spatial uncertainty in mountain water availability (Chen et al. 2018; Uprety et al. 2019). Understanding the sources of water resources in mountainous areas is the basis for water use and

management in these regions and their downstream areas. Considering the important role that K_s plays in runoff generation mechanisms, combined with other measured soil properties and hydrometeorological data, alpine barren contributes the most runoff in mountainous areas, because of the high K_s and low soil water-holding capacity. Although the runoff coefficient is small in the alpine shrub and meadow area, the low K_s and high water-holding capacity would provide the necessary water for the plant growth in this area, which is very important to alpine ecosystems. Forest and marshy meadow are less distributed in the Hulu catchment, and their contribution to runoff is not discussed in detail in this study. Other studies have shown that the forest area in the Qilian Mountains contributes little to the river runoff because of its high canopy interception and evapotranspiration (He et al. 2012; Sun et al. 2016). There are few studies on the hydrological function of marshy meadow or wetlands in the Qilian Mountains. Studies on other high elevation regions showed that marshy meadow had unique hydrological and ecological functions, as a natural water storage and replenishment pool for upstream mountainous catchments (Zha et al. 2012; Shen et al. 2019).

Among the characteristics of high elevation mountainous areas are low temperature and the existence of the cryosphere, which includes glacier, snow and permafrost, which can all influence hydrological processes (Li et al. 2019; Xu et al. 2019). Glacier melt is an important component of runoff in mountainous catchments, and glacial retreats and glacier mass loss under climate changing have dramatically impacted with impact on the runoff of mountainous rivers (Lutz et al. 2014). Snowfall is a common form of precipitation in high elevation mountainous areas, and there is a significant difference between the snowfall and rainfall runoff processes, because of the snowmelt process (Penna et al. 2016). The K_s in permafrost or frozen soil is significantly lower than unfrozen soil (Watanabe and Flury 2008), which can reduce infiltration and permeability and affect the runoff-generated process in cold catchments (Ye et al. 2009; Wang et al. 2019). Because glaciers account for a very small area of the Hulu catchment and most precipitation in this area occurs in the warm season and is mainly rainfall, the influence of the

cryosphere on the runoff generation process is not considered in this study, but it should be addressed in future studies.

4 Conclusions

In this study, the vertical variation of K_s and other soil properties under different land cover types were measured in a small high elevation catchment in the Qilian Mountains. The influence of large-grained soil grain on K_s and other soil properties is significant, and the more rock and gravel in the soil, the higher the K_s and BD and lower CP, FC and TP. The vertical variation of K_s in uniform fine textured or rock and gravel layer is much less than the variation in the clear duplex soil profile, and the CV of the K_s were 1.00, 0.55 and 1.57, respectively. The K_s of lower layers, with mean value of 18.49 mm·min⁻¹, is significantly higher than that in the upper layer, with mean value of 0.18 mm·min⁻¹. The means of the K_s for alpine barren, marshy meadow, forest, alpine shrub and alpine meadow were 17.02 mm·min⁻¹, 0.37 mm·min⁻¹, 11.07 mm·min⁻¹, 0.71 mm·min⁻¹ and 0.15 mm·min⁻¹, respectively, and the values of K_s in the alpine barren were significantly higher than those of other land covers. Under low rainfall intensity,

which was the main rain form in the research catchment, DP was the dominant runoff generation type in the catchment. When the rainfall intensity increased (>0.04 mm·min⁻¹), SSF appeared in the alpine meadow land cover. IOF, SSF and DP existed simultaneously only when the rainfall intensity is large enough to exceed the surface K_s , and it was almost impossible to find IOF and SSF in the alpine barren because of high K_s . The alpine barren contributed the most of the runoff in mountainous areas because of high K_s and low water-holding capacity. Although the runoff coefficient of the alpine shrub and meadow was low, it was very important for mountainous ecological system.

Acknowledgments

This work was carried out with financial support from the National Natural Sciences Foundation of China (Nos. 41401041, 41690141 and 41671029). The authors would like to thank Mr. MA Baoshan for field sampling assistance in the harsh natural environmental condition, and Dr. WANG Lei and Dr. LIU Xiaojiao for the laboratory analysis.

References

- Baetens JM, Verbist K, Cornelis WM, et al. (2009) On the influence of coarse fragments on soil water retention. *Water Resources Research* 45: W07408. <https://doi.org/10.1029/2008wr007402>
- Baiamonte G, Bagarello V, D'Asaro F, et al. (2017) Factors influencing point measurement of near-surface saturated soil hydraulic conductivity in a small Sicilian Basin. *Land Degradation & Development* 28: 970-982. <https://doi.org/10.1002/ldr.2674>
- Becker R, Gebremichael M and Märker M (2018) Impact of soil surface and subsurface properties on soil saturated hydraulic conductivity in the semi-arid Walnut Gulch Experimental Watershed, Arizona, USA. *Geoderma* 322: 112-120. <https://doi.org/10.1016/j.geoderma.2018.02.023>
- Bockgård N, Niemi A (2004) Role of rock heterogeneity on lateral diversion of water flow at the soil-rock interface. *Vadose Zone Journal* 3: 786-795. <https://doi.org/10.2113/3.3.786>
- Chen R, Han C (2010) Hydrology, ecology and climate significance and its research progress of the alpine cold desert (in Chinese). *Advance in Earth Science* 25: 255-263.
- Chen R, Wang G, Yang Y, et al. (2018) Effects of cryospheric change on alpine hydrology: Combining a model with observations in the upper reaches of the Hei river, China. *Journal of Geophysical Research: Atmospheres* 123: 3414-3442. <https://doi.org/10.1002/2017jd027876>
- Chen RS, Song YX, Kang ES, et al. (2014) A cryosphere-hydrology observation system in a small alpine watershed in the Qilian Mountains of China and its meteorological gradient. *Arctic, Antarctic, and Alpine Research* 46: 505-523. <https://doi.org/10.1657/1938-4246-46.2.505>
- Dettinger M (2014) Climate change: Impacts in the third dimension. *Nature Geoscience* 7: 166-167. <https://doi.org/10.1038/ngeo2096>
- Dong L, Zhang M, Wang S, et al. (2015) The freezing level height in the Qilian Mountains, northeast Tibetan Plateau based on reanalysis data and observations, 1979-2012. *Quaternary International* 380-381: 60-67. <https://doi.org/10.1016/j.quaint.2014.08.049>
- Dunne T and Black RD (1970) An experimental investigation of runoff production in permeable soils. *Water Resources Research* 6: 478-490. <https://doi.org/10.1029/WR006i002p00478>
- Fatehnia M, Paran S, Kish S, et al. (2016) Automating double ring infiltrometer with an Arduino microcontroller. *Geoderma* 262: 133-139. <https://doi.org/10.1016/j.geoderma.2015.08.022>
- Fiès JC, Louvigny NDE, Chanzy A (2002) The role of stones in soil water retention. *European Journal of Soil Science* 53: 95-104. <https://doi.org/10.1046/j.1365-2389.2002.00431.x>
- Fu T, Chen H, Zhang W, et al. (2015) Vertical distribution of soil saturated hydraulic conductivity and its influencing factors in

- a small karst catchment in Southwest China. *Environmental monitoring and assessment* 187: 92.
<https://doi.org/10.1007/s10661-015-4320-1>
- Germer K, Braun J (2015) Determination of anisotropic saturated hydraulic conductivity of a macroporous slope. *Soil Science Society of America Journal* 79: 1528–1536.
<https://doi.org/10.2136/sssaj2015.02.0071>
- Chappell NA and Lancaster JW (2007) Comparison of methodological uncertainties within permeability measurements. *Hydrological Processes* 21: 2504–2514.
<https://doi.org/10.1002/hyp.6416>
- Ghimire CP, Bonell M, Bruijnzeel LA, et al. (2013) Reforesting severely degraded grassland in the Lesser Himalaya of Nepal: Effects on soil hydraulic conductivity and overland flow production. *Journal of Geophysical Research: Earth Surface* 118: 2528–2545. <https://doi.org/10.1002/2013jfg02888>
- Ghimire CP, Bruijnzeel LA, Bonell M, et al. (2014) The effects of sustained forest use on hillslope soil hydraulic conductivity in the Middle Mountains of Central Nepal. *Ecohydrology* 7: 478–495. <https://doi.org/10.1002/eco.1367>
- Han C, Chen R, Liu J, et al. (2013) Hydrological characteristics in non-freezing period at the alpine desert zone of Hulugou watershed, Qilian Mountains. (In Chinese) *Journal of Glaciology and Geocryology* 35: 1536–1544.
<https://doi.org/10.7522/j.issn.1000-0240.2013.0170>
- Han C, Chen R, Liu Z, et al. (2018) Cryospheric hydrometeorology observation in the Hulu catchment (CHOICE), Qilian Mountains, China. *Vadose Zone Journal* 17: 180058. <https://doi.org/10.2136/vzj2018.03.0058>
- Hardie MA, Doyle RB, Cotching WE, et al. (2012) Influence of antecedent soil moisture on hydraulic conductivity in a series of texture-contrast soils. *Hydrological Processes* 26: 3079–3091. <https://doi.org/10.1002/hyp.8325>
- Hayashi M (2019) Alpine Hydrogeology: The Critical role of groundwater in sourcing the headwaters of the world. *Groundwater* 58(4): 498–510.
<https://doi.org/10.1111/gwat.12965>
- He Z, Zhao W, Liu H, et al. (2012) Effect of forest on annual water yield in the mountains of an arid inland river basin: a case study in the Pailugou catchment on northwestern China's Qilian Mountains. *Hydrological Processes* 26: 613–621.
<https://doi.org/10.1002/hyp.8162>
- Hlaváčiková H and Novák V (2014) A relatively simple scaling method for describing the unsaturated hydraulic functions of stony soils. *Journal of Plant Nutrition and Soil Science* 177: 560–565. <https://doi.org/10.1002/jpln.201300524>
- Hlaváčiková H, Holko L, Danko M, et al. (2019) Estimation of macropore flow characteristics in stony soils of a small mountain catchment. *Journal of Hydrology* 574: 1176–1187.
<https://doi.org/10.1016/j.jhydrol.2019.05.009>
- Horton RE (1933) The Rôle of infiltration in the hydrologic cycle. *Eos, Transactions American Geophysical Union* 14: 446–460.
<https://doi.org/10.1029/TR014i001p00446>
- Hursh CR and Brater EF (1941) Separating storm-hydrographs from small drainage-areas into surface- and subsurface-flow. *Eos, Transactions, American Geophysical Union* 22: 863–870.
<https://doi.org/10.1029/TR022i003p00863>
- Ilek A, Kucza J (2014) A laboratory method to determine the hydraulic conductivity of mountain forest soils using undisturbed soil samples. *Journal of Hydrology* 519: 1649–1659. <https://doi.org/10.1016/j.jhydrol.2014.09.045>
- Jiang XJ, Liu W, Wu J, et al. (2017) Land degradation controlled and mitigated by rubber-based agroforestry systems through optimizing soil physical conditions and water supply mechanisms: A case study in Xishuangbanna, China. *Land Degradation & Development* 28: 2277–2289.
<https://doi.org/10.1002/ldr.2757>
- Jomaa S, Barry DA, Heng BCP, et al. (2012) Influence of rock fragment coverage on soil erosion and hydrological response: Laboratory flume experiments and modeling. *Water Resources Research* 48: W05535.
<https://doi.org/10.1029/2011wr011255>
- Lai X, Zhu Q, Zhou Z, et al. (2018) Rock fragment and spatial variation of soil hydraulic parameters are necessary on soil water simulation on the stony-soil hillslope. *Journal of Hydrology* 565: 354–364.
<https://doi.org/10.1016/j.jhydrol.2018.08.039>
- Li Z, Feng Q, Li Z, et al. (2019) Climate background, fact and hydrological effect of multiphase water transformation in cold regions of the Western China: A review. *Earth-Science Reviews* 190: 33–57.
<https://doi.org/10.1016/j.earscirev.2018.12.004>
- Lutz AF, Immerzeel WW, Shrestha AB, et al. (2014) Consistent increase in High Asia's runoff due to increasing glacier melt and precipitation. *Nature Climate Change* 4: 587–592.
<https://doi.org/10.1038/nclimate2237>
- Macinnis-Ng CMO, Fuentes S, O'Grady AP, et al. (2010) Root biomass distribution and soil properties of an open woodland on a duplex soil. *Plant and Soil* 327: 377–388.
<https://doi.org/10.1007/s11104-009-0061-7>
- Mohanty BP (2013) Soil hydraulic property estimation using remote sensing: a review. *Vadose Zone Journal* 12: 1–9.
<https://doi.org/10.2136/vzj2013.06.0100>
- Morbiddelli R, Saltalippi C, Flammini A, et al. (2017) In situ measurements of soil saturated hydraulic conductivity: Assessment of reliability through rainfall-runoff experiments. *Hydrological Processes* 31: 3084–3094.
<https://doi.org/10.1002/hyp.11247>
- Mountain Research Initiative EDW Working Group (2015) Elevation-dependent warming in mountain regions of the world. *Nature Climate Change* 5: 424–430.
<https://doi.org/10.1038/nclimate2563>
- Naseri M, Iden SC, Richter N, et al. (2019) Influence of stone content on soil hydraulic properties: experimental investigation and test of existing model concepts. *Vadose Zone Journal* 18: 180163.
<https://doi.org/10.2136/vzj2018.08.0163>
- Page-Dumroese DS, Jurgensen MF, Brown RE, et al. (1999) Comparison of methods for determining bulk densities of rocky forest. *Soil Science Society of America Journal* 63: 379–383.
<https://doi.org/10.2136/sssaj1999.03615995006300020016x>
- Pan T, Hou S, Wu S, et al. (2017) Variation of soil hydraulic properties with alpine grassland degradation in the eastern Tibetan Plateau. *Hydrology and Earth System Sciences* 21: 2249–2261. <https://doi.org/10.5194/hess-21-2249-2017>
- Penna D, van Meerveld HJ, Zuecco G, et al. (2016) Hydrological response of an Alpine catchment to rainfall and snowmelt events. *Journal of Hydrology* 537: 382–397.
<https://doi.org/10.1016/j.jhydrol.2016.03.040>
- Picciafuoco T, Morbiddelli R, Flammini A, et al. (2019) On the estimation of spatially representative plot scale saturated hydraulic conductivity in an agricultural setting. *Journal of Hydrology* 570: 106–117.
<https://doi.org/10.1016/j.jhydrol.2018.12.044>
- Pirastu M, Castellini M, Giadrossich F, et al. (2013) Comparing the hydraulic properties of forested and grassed soils on an experimental hillslope in a Mediterranean environment. *Procedia Environmental Sciences* 19: 341–350.
<https://doi.org/10.1016/j.proenv.2013.06.039>
- Rogora M, Frate L, Carranza ML, et al. (2018) Assessment of climate change effects on mountain ecosystems through a cross-site analysis in the Alps and Apennines. *Science of The Total Environment* 624: 1429–1442.
<https://doi.org/10.1016/j.scitotenv.2017.12.155>
- Ronayne MJ, Houghton TB and Stednick JD (2012) Field characterization of hydraulic conductivity in a heterogeneous alpine glacial till. *Journal of Hydrology* 458–459: 103–109.
<https://doi.org/10.1016/j.jhydrol.2012.06.036>
- Ruiz-Fernández J, Oliva M, Hrbáček F, et al. (2017) Soil temperatures in an Atlantic high mountain environment: The Forcadona buried ice patch (Picos de Europa, NW Spain). *Catena* 149: 637–647.
<https://doi.org/10.1016/j.catena.2016.06.037>

- Scherrer S and Naef F (2003) A decision scheme to indicate dominant hydrological flow processes on temperate grassland. *Hydrological Processes* 17: 391-401. <https://doi.org/10.1002/hyp.1131>
- Schwen A, Zimmermann M and Bodner G (2014) Vertical variations of soil hydraulic properties within two soil profiles and its relevance for soil water simulations. *Journal of Hydrology* 516: 169-181. <https://doi.org/10.1016/j.jhydrol.2014.01.042>
- Shen G, Yang X, Jin Y, et al. (2019) Remote sensing and evaluation of the wetland ecological degradation process of the Zoige Plateau Wetland in China. *Ecological Indicators* 104: 48-58. <https://doi.org/10.1016/j.ecolind.2019.04.063>
- Song X, Yan C, Xie J, et al. (2011) Assessment of changes in the area of the water conservation forest in the Qilian Mountains of China's Gansu province, and the effects on water conservation. *Environmental Earth Sciences* 66: 2441-2448. <https://doi.org/10.1007/s12665-011-1468-z>
- Sun F, Lü Y, Wang J, et al. (2015) Soil moisture dynamics of typical ecosystems in response to precipitation: A monitoring-based analysis of hydrological service in the Qilian Mountains. *Catena* 129: 63-75. <https://doi.org/10.1016/j.catena.2015.03.001>
- Sun F, Lyu Y, Fu B, et al. (2016) Hydrological services by mountain ecosystems in Qilian Mountain of China: A review. *Chinese Geographical Science* 26: 174-187. <https://doi.org/10.1007/s11769-015-0791-9>
- Tian J, Zhang B, He C, et al. (2017) Variability in soil hydraulic conductivity and soil hydrological response under different land covers in the mountainous area of the Heihe River watershed, Northwest China. *Land Degradation & Development* 28: 1437-1449. <https://doi.org/10.1002/ldr.2665>
- Tian J, Zhang B, He C, et al. (2019) Dynamic response patterns of profile soil moisture wetting events under different land covers in the Mountainous area of the Heihe River Watershed, Northwest China. *Agricultural and Forest Meteorology* 271: 225-239. <https://doi.org/10.1016/j.agrformet.2019.03.006>
- Trinh T, Kavvas ML, Ishida K, et al. (2018) Integrating global land-cover and soil datasets to update saturated hydraulic conductivity parameterization in hydrologic modeling. *Science of the Total Environment* 631-632: 279-288. <https://doi.org/10.1016/j.scitotenv.2018.02.267>
- Upreti M, Ochoa-Tocachi BF, Paul JD, et al. (2019) Improving water resources management using participatory monitoring in a remote mountainous region of Nepal. *Journal of Hydrology: Regional Studies* 23: 100604. <https://doi.org/10.1016/j.ejrh.2019.100604>
- Verbist KMJ, Cornelis WM, Torfs S, et al. (2013) Comparing methods to determine hydraulic conductivities on stony soils. *Soil Science Society of America Journal* 77: 25-42. <https://doi.org/10.2136/sssaj2012.0025>
- Wang X, Chen R, Liu G, et al. (2019) Response of low flows under climate warming in high-altitude permafrost regions in western China. *Hydrological Processes* 33: 66-75. <https://doi.org/10.1002/hyp.13311>
- Watanabe K and Flury M (2008) Capillary bundle model of hydraulic conductivity for frozen soil. *Water Resources Research* 44: W12402. <https://doi.org/10.1029/2008wr007012>
- Xu M, Kang S, Wang X, et al. (2019) Understanding changes in the water budget driven by climate change in cryospheric-dominated watershed of the northeast Tibetan Plateau, China. *Hydrological Processes* 33: 1040-1058. <https://doi.org/10.1002/hyp.13383>
- Yang Y, Chen R, Song Y, et al. (2017) Comparison experimental study on double-ring infiltrometers with different sizes in the Qilian Mountain. *Journal of Soils and Water Conservation* 31: 328-331, 336. <https://doi.org/10.13870/j.cnki.stbxb.2017.01.054>
- Ye B, Yang D, Zhang Z, et al. (2009) Variation of hydrological regime with permafrost coverage over Lena Basin in Siberia. *Journal of Geophysical Research* 114: D07102. <https://doi.org/10.1029/2008jd010537>
- Zha X, Huang D, Gu M, et al. (2012) Study on forty-year snow cover of Zoige Plateau. *Plateau and Mountain Meteorology Research* 32: 61-64.
- Zhang Y and Schaap MG (2019) Estimation of saturated hydraulic conductivity with pedotransfer functions: A Review. *Journal of Hydrology* <https://doi.org/10.1016/j.jhydrol.2019.05.058>
- Zhang Y, Zhang M, Niu J, et al. (2016) Rock fragments and soil hydrological processes: Significance and progress. *Catena* 147: 153-166. <https://doi.org/10.1016/j.catena.2016.07.012>
- Zhi J, Zhang G, Yang F, et al. (2017) Predicting mastic epipedons in the northeastern Qinghai-Tibetan Plateau using Random Forest. *Geoderma Regional* 10: 1-10. <https://doi.org/10.1016/j.geodrs.2017.02.001>
- Zhou H, Zhao W and Yang Q (2016) Root biomass distribution of planted Haloxylon ammodendron in a duplex soil in an oasis: desert boundary area. *Ecological Research* 31: 673-681. <https://doi.org/10.1007/s11284-016-1376-5>
- Zimmermann B and Elsenbeer H (2009) The near-surface hydrological consequences of disturbance and recovery: A simulation study. *Journal of Hydrology* 364: 115-127. <https://doi.org/10.1016/j.jhydrol.2008.10.016>
- Zimmermann B, Elsenbeer H and De Moraes JM (2006) The influence of land-use changes on soil hydraulic properties: Implications for runoff generation. *Forest Ecology and Management* 222: 29-38. <https://doi.org/10.1016/j.foreco.2005.10.070>